

Performance & Analysis of Blocking & Ringing Artifacts Reduction Using Generalized Least Square (GLS) Algorithm

*M. Anto Bennet, G. Vijayalakshmi, P. Maragathavalli,
S. Lokesh and T.R. Dinesh Kumar*

Department of Electronics and Communication Engineering,
VELTECH, Avadi-Chennai- 600062, Tamilnadu, India

Abstract: Traditional block-based video coders such as H.261, MPEG-1 and MPEG-2 suffer from annoying blocking artifacts when they are applied in low bit-rate coding because inter block correlation is lost by block-based prediction, transformation and quantization. In order to overcome the blocking artifact problem, various non block-based coding schemes are used. In Existing Artifact Reduction method, the quality of astrophysical images produced by means of the generalized least square (GLS) approach may be degraded by the presence of artificial structures, obviously not present in the sky. In this paper, we analyze these artifacts and introduce a method to remove those using GLS and Feature extraction techniques. The method is based on a post-processing of GLS image that estimates and removes the artifacts subtracting them from the original image. The method we present here is termed post-processing for GLS (PGLS) and is based on an artifact estimation procedure. Once the artifacts are estimated, they are subtracted from the GLS image to produce a clean image. The PGLS algorithm is simple and robust. Its computational complexity is affordable and comparable to that of the GLS map maker itself. The Proposed method will be compared with existing approach.

Key words: Generalized least square (GLS) approach • Blocking & Ringing Artifacts • Peak signal to Noise Ratio(PSNR) • Deblocking filter

INTRODUCTION

The quality of astrophysical images produced by means of the generalized least square (GLS) approach may be degraded by the presence of artificial structures, obviously not present in the sky. This problem affects, in different degrees, all images produced by the instruments onboard the European Space Agency's Herschel satellite. Existing method, they analyze these artifacts and introduce a method to remove them. The method is based on a post-processing of GLS image that estimates and removes the artifacts subtracting them from the original image. The only drawback of this method is a slight increase of the background noise which, however, can be mitigated by detecting the artifacts and by performing the subtraction only where they are detected. The efficiency of the approach is demonstrated and quantified using simulated and real data. In existing method the artifact will be removed by using De-blocking Filtering Method and

trilateral filtering method. In contrast with older MPEG-1/2/4 standards, the H.264 de-blocking filter is not an optional additional feature in the decoder. It is a feature on both the decoding path and on the encoding path, so that the in-loop effects of the filter are taken into account in reference macroblocks used for prediction. When a stream is encoded, the filter strength can be selected, or the filter can be switched off entirely. Otherwise, the filter strength is determined by coding modes of adjacent blocks, quantization step size and the steepness of the luminance gradient between blocks. The filter operates on the edges of each 4×4 or 8×8 transform block in the luma and chroma planes of each picture. Each small block's edge is assigned a boundary strength based on whether it is also a macroblock boundary, the coding (intra/inter) of the blocks, whether references (in motion prediction and reference frame choice) differ and whether it is a luma or chroma edge. Stronger levels of filtering are assigned by this scheme where there is likely to be more distortion.

The filter can modify as many as three samples on either side of a given block edge (in the case where an edge is a luma edge that lies between different macroblocks and at least one of them is intra coded). In most cases it can modify one or two samples on either side of the edge (depending on the quantization step size, the tuning of the filter strength by the encoder, the result of an edge detection test and other factors).

Related Work: Rourke, T.P.O. and Stevenson, R.L. [1] had Proposed for Binary arithmetic Coding, Probability estimation. Adaptive Binary Arithmetic Coding with Context modeling, high degree of adaptation and redundancy reduction technique is used. Shapiro, J. and Apostolopoulos, T. [2] had proposed a block boundaries an adaptive approach which performs blockiness in both DCT and spatial domain to reduce the block –block discontinuous. In this it has a major drawbacks of the block based may result in a visible artifacts. Shohdohiji, T. [3] had Proposed for Novel method to quantify blur and ringing artifact in an image. Objective Quality Assessment, Compression, Ringing Artifacts technique is used. Sung Cheol Park, [4] had proposed quantization noise with high resolution data, blocking and ringing artifacts. DCT based compression, high resolution is used. Tasi, R.Y. and Huang, T.S. [5] had Proposed Projections onto convex sets (POCS), Constrained Least Square (CLS), Iterative algorithms, Regularized Re-Construction technique is used. Watabe, H. and Ara'kawa, Y. [6] had proposed for Coding artifacts in Transform image coding, Low bit-rate coded images. Theory of Projections onto Convex sets (POCS) and Maximum a Posteriori (MOP) estimation technique is used. Westen, S.J.P. and Lagendijk, R.L. [7] had Proposed for Mean Square Error (MSE), Block edge Impairment Metric (BIM), Reducing Blocking artifacts in decoded image. Content Adaptive Filtering, De-blocking, JPEG, MPEG, Local Image pattern or Relative pixel location technique is used. Xinghao Jiang and Michael, [8] had proposed for powerful and easy to easy video dining software, digital videos are exposed to various forms of tampering. In this double compression techniques used in this paper.

Yang, Y. and Galatsano, N. [9] had Proposed for Removal algorithm that is Adaptive to the Artifact visibility level of the input video signal was proposed. Adaptive filters techniques are used in adaptive LPF. Ying Luo and Rabab, k. [10] had proposed a block boundaries an adaptive approach which performs

blockiness in both DCT and spatial domain to reduce the block –block discontinuous. In this it has a major drawbacks of the block based may result in a visible artifacts. Yonghi Yang, [11] had proposed a multichannel regularized recovery approach to ameliorate coding artifacts in compressed video. The major advantage of the proposed approach is that both temporal and spatial correlations in a video sequence can be exploited to complement the compressed video data. Yongi Yong, [11] had proposed the image in the artifacts can be removed by using Projections Onto the Convex Sets (POCS) and by using modeling methods. In this method, which uses a new image recovery algorithm to remove, in addition to blocking, ringing artifacts from compressed images and video. Yuen, M. and Wu, H.R. [12] had Proposed for powerful and easy-to-easy video coding software, digital videos are exposed to various forms of Tampering. double compression techniques was used. Zakhori, A. [13] had Proposed that it significantly reduces the blocking artifact of still video image, as judged by both objective and subjective measures. DCT and spatial domain is used to reduce the block-to-block discontinuities. MPEG technique is used. Zhao, M. [14] had proposed that the blocking artifacts in the block based digital image and the video coding system like JPEG and MPEG especially compressed and it is done at a low bit rate. The selection of the proper filter is based on the local image pattern in the coding block. In this both mean square error and block edge impairment metric error can also occur. Zhen Li Sch *et al* [15] had proposed for block based Discrete Cosine Transform (DCT) is often used in image and video coding. It may introduce block artifacts at low rates that manifest themselves as an annoying discontinuity between adjacent blocks. The experimental results confirm that TSD-MR can improve visual quality both objectively and subjectively over SD-MRF methods.

Proposed System: In our proposed system we introducing GLS Algorithm based feature extraction for artifact reduction in satellite images. The Existing system removes only blocking artifact, but in our proposed system removes blocking as well as ringing artifact from the artifact satellite images. And the performance of the satellite image also will be analyses in the proposed system. By using the GLS artifact reduction technique the artifacts from the satellite images as well as medical images are removed. Then the performance of the image will be calculated by using the evaluation of the PSNR value [16].

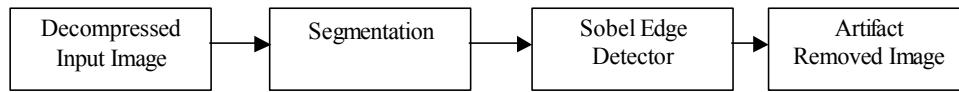


Fig. 1: Block Diagram of GLS Implementation

GLS Implementation: The first one, termed Post-processed GLS (PGLS), is based on an artifact estimation algorithm. Once the artifacts are estimated they can be subtracted from the GLS image to produce a clean image. The PGLS algorithm is simple and robust. Its computational complexity is affordable and comparable to that of the GLS map maker itself. The only drawback is that, when the artifacts are subtracted, some noise is also added to the image. However the noise increase is normally moderate and the cleaned image is surely more useful than the original GLS one. Segmentation is a procedure that partitions an image into multiple regions, each of which is uniform or similar in certain characteristics. Document images are often segmented into regions, such as text, synthetic graphics and natural pictures for various purposes. The result of image segmentation is a set of segments that collectively cover the entire image, or a set of contours extracted from the image (see edge detection). Each of the pixels in a region is similar with respect to some characteristic or computed property, such as color, intensity, or texture. Adjacent regions are significantly different with respect to the same characteristic(s). When applied to a stack of images, typical in medical imaging, the resulting contours after image segmentation can be used to create 3D reconstructions with the help of interpolation algorithms like Marching cubes. There are many types of image segmentation. Here we are using edge detection segmentation process is shown in Fig 1.

System Implementation- GLS Algorithm: Map making is the process of constructing an image from a sequence of geo referenced (or sky referenced) data. A map maker is an algorithm employed to perform the process. An excellent map maker for astronomical images is the one based on the Generalized Least Square (GLS) approach. Indeed GLS map makers proved effective in removing the noise affecting the data sequence and have a manageable computational complexity, which makes their use feasible even on the huge amount of data produced by current days imaging photometers, like the PACS and SPIRE instruments onboard the ESA Herschel satellite. Furthermore the GLS approach has nice features from a theoretical point of view. In fact it is a linear algorithm and

therefore amenable to analysis and it can be shown to yield the maximum likelihood (ML) map when the noise affecting the data is a Gaussian process. However the approach also has a serious drawback that became apparent when it was employed to process the data gathered within the HiGal project, the aim of which is that of performing a survey of the galactic plane. Namely it introduces artifacts in the form of crosses or stripes on strong point sources. These artifacts are annoying and make the resulting images of little interest, which is a pity since, as we said, the GLS approach is otherwise a very good map maker. Therefore a procedure to cure this problem is of both theoretical and practical interest. In this report we present two such procedures.

The first one, termed Post-processed GLS (PGLS), is based on an artifact estimation algorithm. Once the artifacts are estimated they can be subtracted from the GLS image to produce a clean image. The PGLS algorithm is simple and robust. Its computational complexity is affordable and comparable to that of the GLS map maker itself. The only drawback is that, when the artifacts are subtracted, some noise is also added to the image. However the noise increase is normally moderate and the cleaned image is surely more useful than the original GLS one. The second one, termed Split GLS (SGLS), is based on splitting the signal into a diffuse emission plus correlated noise part and a point sources plus white noise part. Then, the diffuse part is mapped with GLS, the point source part is mapped by simple rebinning and the SGLS image is obtained by summing the two maps. Also the SGLS algorithm is simple and robust. Its computational complexity is essentially that of the GLS map maker itself. Also SGLS introduces some additional noise, but less than PGLS. However the signal seems to be reconstructed not as well as by PGLS.

Data, Map & Pointing: To be specific we consider the map making problem as it arises in the processing of the data produced by the scan mode of the PACS instrument of the Herschel satellite. The instrument is composed of a grid of Nb bolometers and a scan amounts at pointing the instrument towards a set of Nk given points in the sky (organised into a grid of parallel lines) and at sampling the bolometers output at each point. The result is a set of time

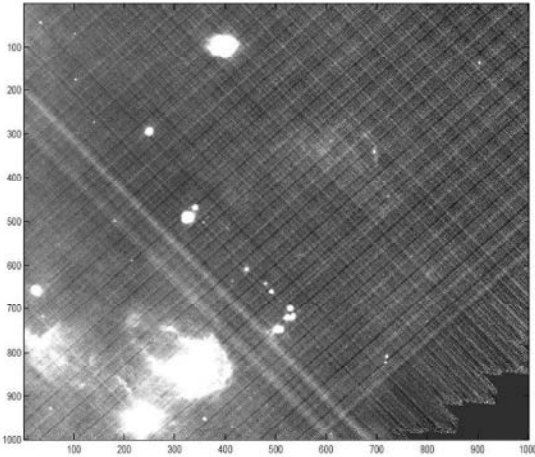


Fig. 2: Rebinning from a TOD of PACS blue, tile L323

ordered data (TOD) which will be denoted by $t = \{t_b, k\}$ for $b = 1, N_b$ and $k = 1, N_k$, where t_b, k is the readout of the b -th bolometer at the k -th scan point. Each readout is accompanied by a sky referencing information, which is a pair (x_b, k, y_b, k) giving the right ascension and the declination of the readout. The map making problem is that of constructing an image (map) of the observed sky from the TOD. The typical approach is that of defining a pixelization of the observed sky, i.e. partitioning the sky into a grid of $N_i \cdot N_j$ non overlapping squares (pixels) s_i, j . The map maker has to produce a map $m = \{m_{i,j}\}$ where $m_{i,j}$ is a measure of the flux in s_i, j , i.e. in the (i, j) -th pixel. We will see several map makers in the following sections. To conclude this section let us note that since each readout is skyreferenced and assuming that the pixelization covers the whole observed sky, we can assign each readout (b, k) to one and only one pixel. Therefore we can introduce a pointing function $P_{b,k}$ yielding the pixel (i, j) where the readout (b, k) was taken. In other words $P_{b,k} = (i, j)$ if and only if $(x_b, k, y_b, k) \in s_{i,j}$. Conversely, for each pixel (i, j) we can consider the (possibly void) set of readouts falling in the pixel and denote this set by $C_{i,j}$. Formally we have $C_{i,j} = \{(b, k) | P_{b,k} = (i, j)\}$. Furthermore we will denote by $|C_{i,j}|$ the number of elements of $C_{i,j}$, that is the number of readouts falling in pixel (i, j) .

Rebinning & Unrolling: Rebinning is a simple and important map making technique where the value of each pixel is set equal to the mean value of all the readouts falling in the pixel. Namely, the map is computed as

$$m_{i,j} = \frac{1}{|C_{i,j}|} \sum_{(b,k) \in C_{i,j}} t_{b,k}. \quad (1)$$

Rebinning is simple, robust and computationally cheap. It does not require any prior knowledge about the noise affecting the TOD. Moreover, it is also the optimum solution when the TOD is a made by a signal affected by zero mean, white noise, in the sense that it yields the ML map and maximizes the SNR. However when the noise affecting the TOD is coloured, rebinning is no more optimum. Unfortunately the bolometer are typically affected by coloured noise, having a power spectrum that grows as $1/f$ for $f \neq 0$. As a result the maps obtained by rebinning the TOD are not of good quality. An example is shown in Fig 2 where the rebinning for a patch of tile L323 in the PACS blue band is shown. The effect of the $1/f$ noise is apparent and manifests itself as stripes following the scan directions. Nevertheless rebinning is an important tool in map making and it will be useful in the following.

A second operation that we will need in the following is the unrolling of a map into a TOD. This operation assumes that a map m is given and that the pointing function $P_{b,k}$ is assigned. It then produces the TOD data by unrolling the map onto the TOD. Specifically, the data of each readout is set equal to value of the pixel where the readout falls. Therefore, the unrolled TOD is given by $t_{b,k} = m_{P_{b,k}}$.

GLS Map Making: GLS map making, in its simplest form, is based on the following model for the TOD

$$t = U(m) + n \quad (2)$$

where, $n = \{n_{b,k}\}$ is a noise affecting the TOD. The last equation models the TOD as obtained by unrolling a map (the sky) onto a TOD and by adding noise to it. Based on this model, the approach exploits the GLS technique and seeks for a map m_g minimising the Weighted sum of the squared noise estimate, given by $t - U(m_g)$. By properly selecting the weights and specifically, by setting them based on the noise covariance matrix, one can show that the resulting map m_g is the minimum variance linear estimator of m . Furthermore, when the noise is Gaussian, m_g is also the ML estimate of m . GLS map making is a sophisticated and effective map making technique. While it is more complex than the rebinning, its computational complexity can be kept manageable by exploiting the Conjugate Gradient approach to obtain the solution map. It requires the knowledge of the noise correlation properties or, what is equivalent, of the noise power spectrum. However simulations show that it is robust to

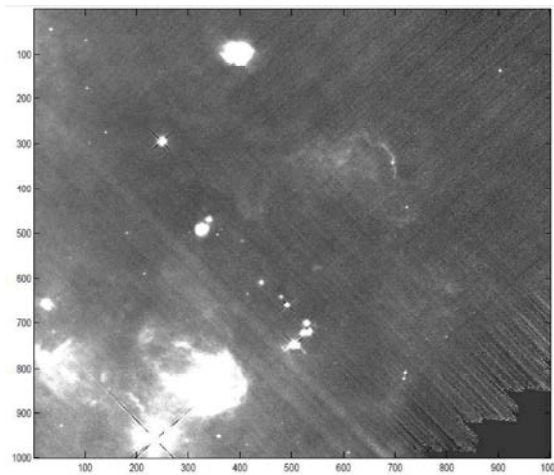


Fig. 3: GLS map from Tile L323 for the PACS blue band

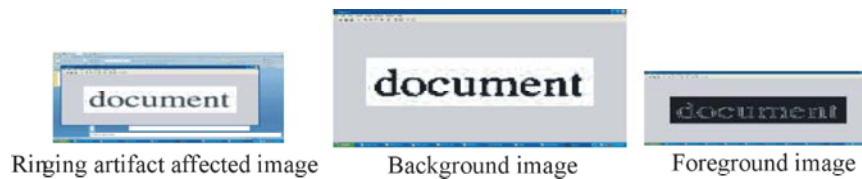


Fig. 4: Result of Thresholding

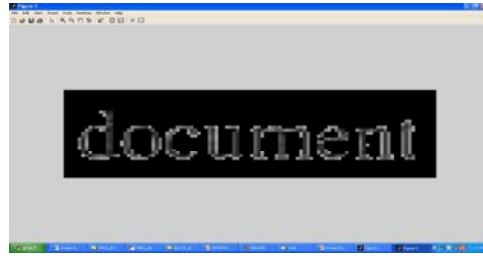
a mismatch between the spectrum employed in the solution and the actual spectrum. Its main advantage is that it keeps into account the noise correlation and is therefore capable of removing the $1/f$ noise and of producing much better maps than the rebinning. However it also has a major drawback, namely that it introduces artifacts in the form of crosses centered on bright point sources, with arms parallel to the scan directions. An example of GLS map is shown in Fig 3 where one notes both the absence of the stripes due to the $1/f$ noise and the artifacts. The artifacts are due to the fact that the model of is not correct and neglects several important facts. The core mismatch of the model from the actual physical process is that the TOD is not produced by unrolling a pixellised sky. On the contrary it is produced by taking samples over a continuous sky. This mismatch is not a problem when the sky is a smooth, slowly varying image, like happens with diffuse emissions or large, wide sources. However for pointed, bright sources the mismatch is relevant. Two additional mismatches are 1) the fact that the in the PACS instrument, in order to improve the SNR while reducing the data rate, the TOD are obtained by coadding and subsampling a higher resolution TOD and 2) the fact that the TOD is affected by a small Relative Pointing Error (RPE). By means of simulations it was verified that any of these three factors causes the artifacts observed in the GLS maps. To

conclude let us note that, in principle, the model of can be improved to obtain an artifact-free GLS approach. This can be done also in practice, at least approximately, for the artifacts due to the RPE, which can be estimated and removed. And for the artifacts due to the coaddition, following the approach proposed in. However improving the model to keep into account the continuous nature of the sky would require to change the pointing matrix used in the implementation of the GLS algorithm from a sparse one to a fully populated one. Such a change would increase the computational complexity of the GLS algorithm dramatically, making it unfeasible with current days processing power.

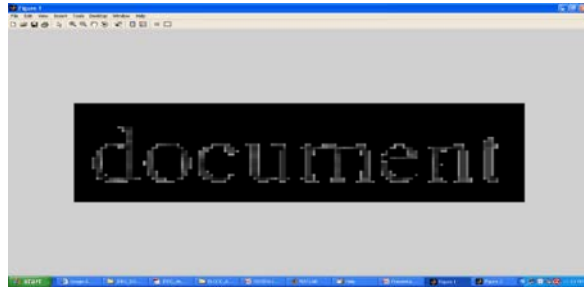
Experimental Results: The Fig. 4 shows that the output of thresholding process, when the ringing atrifacted image will be given as input in the matlab tool. The Fig.5 shows that the result of the eroded process, by eroded the image by factor 3.

The Fig. 6 shows the output of segmentation process with edge detection technique. The ringing artifact reduced image will be shown in the Fig. 7. Here the ringing artifact affected image was taken as input.

The result of blocking artifact reduced image will be shown in the Fig. 8. Here the blocking artifacted image will be given as input.



Foreground image



Eroded image by factor 3

Fig. 5: Eroded process



Fig. 6: Segmentation process



Fig. 7: Ring Artifact Reduction

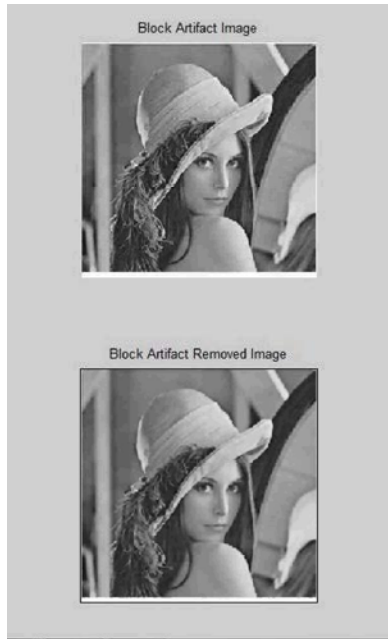


Fig. 8: Block Artifact Reduction

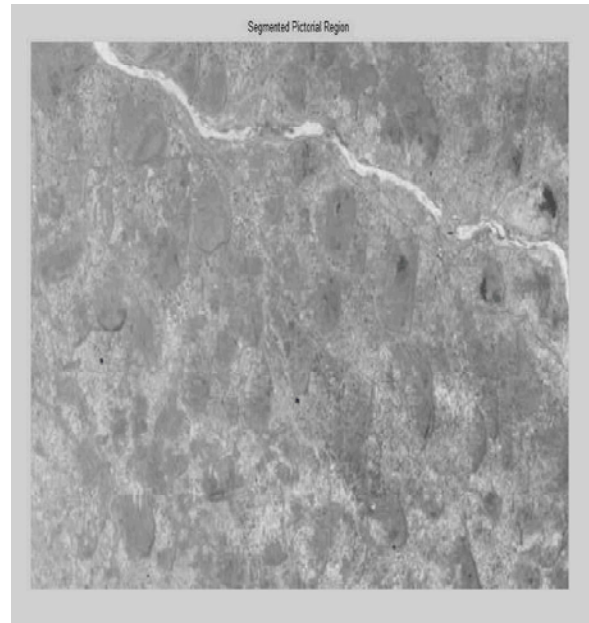


Fig. 10: Segmented Pictorial Image



Fig. 9: Input Astrophysical Image



Fig. 11: Block Artifact Image Fig 12.Edge Detected Image

Artifact Reduction Using GLS Algorithm: The result of artifact reduction using the GLS algorithm will be shown in the following figures. The Fig 9 shows that an decompressed astrophysical input image.

The Fig 10 shows the segmented Pictorial Region of the input image. This Process is done by segmentation method. The Figure11 Shows that the block artifact image, which contains only the pictorial or natural image region.

The Figure 12 shows that the edge detected image. Here the Edge detection is done by using the Sobel Operator. Finally the Figure 13 shows the artifact removed astrophysical image. Here both of the ringing and blocking artifacts will be removed from the image.

In our simulation (Shown in Table 1), we have performed the JPEG images with the different characters and the quality factor QF to evaluate



Fig 12.Edge Detected Image

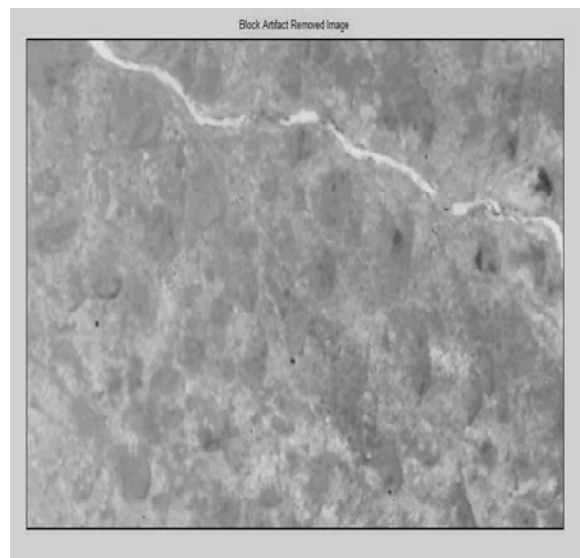


Fig. 13:Artifact Removed Image

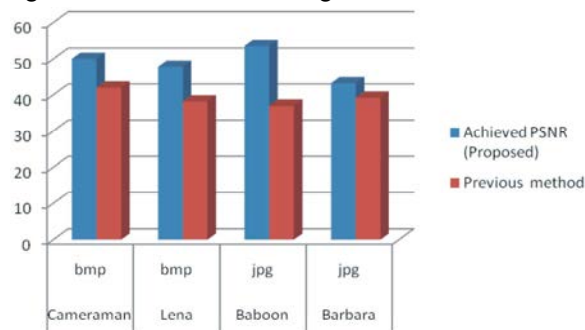


Fig. 14:Performance of PSNR Compared with the Existing System

Table 1: Comparison table of PSNR values

Image Name	Image Type	Achieved PSNR (Proposed)	Previous method
Cameraman	bmp	50	42
Lena	bmp	47.8	38.2
Baboon	jpg	53.6	37
Barbara	jpg	43.2	39.2

our proposed method. In the parameter σ_r of range filter used in our simulations is 30 if $G_{max} > 950$; $\sigma_r = 10$ or otherwise.

PSNR is most commonly used to measure the quality of reconstruction of lossy compression codecs (e.g., for image compression). The signal in this case is the original data and the noise is the error introduced by compression. When comparing compression codecs, PSNR is an approximation to human perception of reconstruction quality. Although a higher PSNR generally indicates that the reconstruction is of higher quality, in some cases it may not. One has to be extremely careful with the range of validity of this metric; it is only conclusively valid when it is used to compare results from the same codec (or codec type) and same content is shown in Fig 14.

CONCLUSION

Traditional block-based video coders such as H.261, MPEG-1 and MPEG-2 suffer from annoying blocking artifacts when they are applied in low bit-rate coding because inter block correlation is lost by block-based prediction, transformation and quantization. In order to overcome the blocking artifact problem, various non block-based coding schemes are used. In Existing Artifact Reduction method, the quality of astrophysical images produced by means of the generalized least square (GLS) approach may be degraded by the presence of artificial structures, obviously not present in the sky. There are two types of artifacts occur in the astrophysical images, due to image compression. They are blocking artifacts and ringing artifact. In which, by using a post processing method the blocking artifacts and ringing artifacts are removed from the astrophysical images. The compressed input image will be processed with the post processing method and both of the ringing and blocking artifacts will be removed. And the expected image clarity was occurring with more efficient than, when compared to the existing artifact removing method. Then the remaining amount of artifacts occur in the image will be removed by using the GLS algorithm. And the better PSNR value will be achieved, in order to improve the quality of the image.

REFERENCES

1. Rourke, T.P.O. and R.L. Stevenson, 2011. Improved Image Decompression For Reduced Transform Coding Artifacts, *IEEE Trans,Circuits Syst. Technol.*, 5(5): 490-409.
2. Shapiro, J. and T. Apostolopoulos, 2010. Image coding based on a fractal theory of iterated contractive, 5(8): 34-37.
3. Shohdohiji, T., 2011. Method and Apparatus For The Reduction of Mosquito Noise in Decoded Images, *IEEE Transaction on Image Processing*, 13(9): 980-990.
4. Sung Cheol Park, 2010. Spatially Adaptive High Resolution Image Reconstruction of DCT-Based Compression Image, *IEEE Transaction on Image*, 43(2): 565-587.
5. Tasi, R.Y. and T.S. Huang, 2013. Multiple Frame Image Restoration and Registration, *IEEE Transaction on image Processing*, 34(7): 257-289.
6. Watabe Hand, Y. and Arakawa, 2010. Nonlinear Filters for Multimedia Application, in *IEEE int.conf.Image Processing*, 7(2): 876-890.
7. Westen, S.J.P. and R.L. Lagendijk, 2010. Adaptive Spatial Noise Shaping For Dct Based Image Compression, *IEEE Transaction on*, 49(1): 229-236.
8. Xinghao Jiang and Michael, 2010. Detection of Double Compression in MPEG-4 Video Based on Markov Statistics, *IEEE Transaction on Image Processing*, 16(3): 456-567.
9. Yang, Y. and N. Galatsano, 2011. Regularized Reconstruction to Reduce Blocking Artifacts of Block Discrete Cosine Transform Compressed Image, *IEEE Transactions on Circuits and System for Video Technology*, 3(6): 421-432.
10. Ying Luo and k. Rabab, 2010. Removing The Blocking Artifacts of Block-Based DCT Compressed Images, *IEEE Transaction on Image Processing*, 12(7): 789-890.
11. Yongyi Yang, 2011. Multichannel Regularized Recovery of Compressed Video Sequences, 25(6): 5678-987.
12. Yongyi Yang, P. Nikolas and D. Donoho, 2011. Removal of Compression Artifacts Using Projections onto Convex Sets and Line Process Modeling, *IEEE Transaction on Image Processing*, 6(10): 789-790.
13. Yuen, M. and H.R. Wu, 2010. An Efficient Multipliers Algorithm for Video Coding, 7(1): 247-278.
14. Zakhori, A., 2010. Reduction of Blocking Effect in Image Coding, *IEEE Transaction on Image Processing*, 8(14): 134-234.
15. Zhao, M., 2010. Content Adaptive Image De-Blocking, *IEEE Transaction on Image Processing*, 24(9): 345-567.
16. Zhen Li Sch, P. Crouch and M. Shapiro, 2010. Block Artifact Reduction Using a Transform Domain Markov Random Field Model, *IEEE Transaction on Image Processing*, 7(8): 456-478